J Appl Electrochem (2010) 40:1839–1844
DOI 10.1007/s10800-010-0111-0

ORIGINAL PAPER

The effect of CVD-diamond film thickness on the electrochemical properties of synthetic diamond thin-film electrodes

M. D. Krotova · Yu. V. Pleskov · V. P. Varnin · I. G. Teremetskaya

Received: 22 October 2009 / Accepted: 12 March 2010 / Published online: 12 June 2010

Abstract The electrochemical behavior of polycrystalline diamond films of different thickness (0.5–7 μm), grown by hot-filament CVD method, was studied by electrochemical impedance spectroscopy and cyclic voltammetry. The differential capacitance, background current, and potential window were measured in supporting electrolyte solution; the electrochemical kinetics, in $[Fe(CN)_6]^{3-/4-}$ model redox system. With the increasing of the films thickness, the crystallite size increased; both the differential capacitance and background current in the indifferent electrolyte, as well as the transfer coefficients in the redox system, decreased; thus, the diamond electrode becomes as if less reversible. The effect of the films' thickness is reduced to that of nondiamond (amorphous) carbon contribution from intercrystalline boundaries on the electrochemical behavior of the polycrystalline diamond electrodes.

Keywords CVD-diamond · Thin films · Nondiamond carbon · Intercrystalline boundaries · Differential capacitance · Background current

Dedicated to Professor Christos Comninellis on the occasion of his 65th birthday.

M. D. Krotova · Yu. V. Pleskov (✉) · V. P. Varnin · I. G. Teremetskaya
Frumkin Institute of Physical Chemistry and Electrochemistry, Russian Academy of Sciences, Leninskii pr. 31, Moscow, Russia 119991
e-mail: pleskov@electrochem.msk.ru

1 Introduction

The effect of crystal structure of chemical-vapor-deposited (CVD) diamond thin films on their electrochemical behavior is studied rather thoroughly [1–3]. Possible specific contribution of sp^2-carbon inclusions to electrochemical properties of polycrystalline diamond is widely discussed in literature, in particular, by Comninellis and coworkers [4, 5]. Comparative studies of the double-layer structure and kinetics of electrochemical reactions proceeding in numerous redox couples showed that single crystal and polycrystalline diamond electrodes are close to each other as regards their kinetic characteristics, at least, at moderate polarization. It was concluded [1] that intercrystalline boundaries, constituted by disordered carbon, do not contribute, to the first approximation, to the electrode behaviour of polycrystalline diamond, which is mainly determined by diamond crystallites proper. However, the intercrystalline boundaries sometimes manifest themselves in the shape of potentiodynamic curves [6]. There is a short report on some connection between the CVD-diamond film thickness and the electrochemical behavior [7]. Also, worth mentioning are the studies of nanocrystalline diamond films containing diamond nanosized grains plunged into amorphous carbon continuous matrix; the effect of the "intercrystalline boundaries" on the physical, electrical (first and foremost, the electrical conductance), and electrochemical properties become ever more pronounced [8, 9].

In this work we have grown a series of CVD-diamond thin-film electrodes and studied their properties in indifferent electrolyte and redox-system as a function of the film thickness.

2 Experimental

2.1 Deposition of diamond films

Polycrystalline diamond films were grown by hot-filament CVD (HFCVD) method using methane–hydrogen mixture as a carbon source. The deposition of diamond was carried out in a stainless steel reactor provided with quartz windows in the housing's wall and bottom. Substrates for deposition of diamond films were placed onto the water-cooled horizontal copper sample holder. The temperature of the holder was measured by a thermocouple.

Close to the holder surface, a tungsten activator was mounted. The activator is a row of tungsten rods parallel to the holder surface, heated by the passing electrical current. The tungsten rod temperature was measured by an optical pyrometer through the quartz window. The temperature of the samples was measured by another optical pyrometer through the narrow cylindrical channel in the holder and the quartz window located at the bottom of the reactor.

The temperature of the tungsten rods was $\sim$2000 °C; the substrate temperature was kept in the range from 860 to 890 °C. The total gas pressure was 30–36 Torr. The methane content in the gas phase was kept near 1.2%. Balloon gases were used as sources of pure hydrogen and methane. The gas flow rates were adjusted and maintained by automatic flow controllers.

To produce conducting films, the diamond was doped with boron during the deposition. For this purpose, vapor of a trimethyl borate solution was added to the methane–hydrogen gas mixture. To prepare the solution, trimethyl borate was dissolved in methanol and then acetone was added, to adjust the boron concentration. The calculated relative concentration of B/C in the feeding gas varied in 2500–3500 ppm range.

Unpolished boron-doped *p*-type silicon plates ($12 \times 12 \times 1$ mm^3) with resistivity of 10 Ohm cm were used as substrates.

Prior to the diamond deposition, the silicon substrates were "pre-seeded", to enhance the diamond nucleation and to ensure getting of *continuous* diamond films of micron thickness. The pre-seeding was performed in ultrasonic bath with suspension of nanodiamond powder in acetone or by the polishing of the substrates by a paste containing the nanodiamond powder. The average thickness of diamond films was calculated from the diamond mass gain, by weighing the substrates before and after diamond deposition. In the calculations, the diamond density was thought of as thickness-independent. Indeed, even thinnest films ($\sim$0.5 μm) are very dense, free of pinholes and other structural macrodefects.

Prior to electrochemical experiments, the as-grown diamond films were annealed in air at 520 °C for 40–50 min, to remove the film of nondiamond (amorphous) carbon that might form on top of the crystalline diamond film during the last, poorly controlled stages of the diamond film growth.

2.2 Film characterization

2.2.1 SEM images

A number of thin-film diamond samples with average thickness from 0.5 to 7 μm were prepared. In Fig. 1 SEM pictures of the diamond films of different thickness are presented.

One can conclude that the diamond grain average size observable on the film surface increases with the film thickness. The approximate estimation of the average visible lateral crystallite size was carried out by the counting of the crystallite number per unit length; the results are given in Table 1.

Concerning the film morphology, we see the prevailing of diamond crystallites with well pronounced crystal facets having different crystallographic orientations.

2.2.2 Raman spectra

The Raman spectroscopy is a preferable tool for identification of diamond, evaluation of the diamond film crystallinity, and detection of the nondiamond carbon impurity. Undoped diamond is rather transparent a material; hence, the Raman spectroscopy gives the integral information about the properties of diamond layer up to 5–6 μm thick. For highly doped diamond this value is less because of the decrease of the diamond transparency.

Raman spectra of diamond films with different thickness are given in Fig. 2. For diamond single crystals, the distinctive feature of the Raman spectra is the presence of a strong narrow peak at 1332 cm^{-1}. In the spectra of our highly doped polycrystalline films, the peak position still remains at 1332 cm^{-1}. We see that the diamond peak is well pronounced for all film thicknesses. While the nondiamond carbon maximum at $\sim$1550 cm^{-1} becomes ever weaker with the increasing of the film thickness. Below we shall come back to this point.

2.3 Electrochemical measurements

Electrochemical glass cell comprised a working diamond electrode and a platinum auxiliary electrode; the anodic and cathodic compartments were not separated. The interelectrode space between the working and auxiliary electrodes is 5–7 mm. In electrochemical measurements, the substrate with a film was pressed up to a polished flange of a round opening in the glass wall of the electrochemical

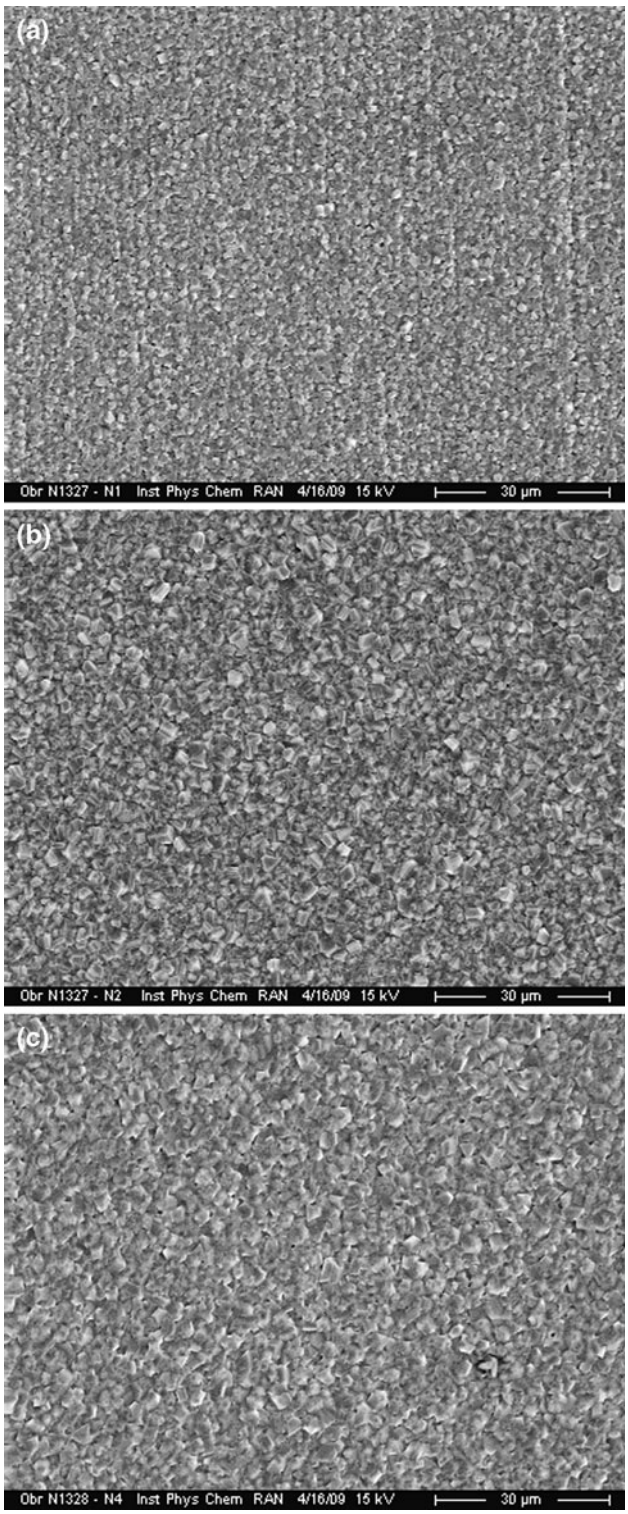

Fig. 1 SEM photomicrographs of diamond films of different thickness (μm): **a** 2.3; **b** 3.6; **c** 4.2

cell. A silicon-rubber O-ring was used as a gasket; the working surface area was ~0.2 cm^2. The electrical contact to the silicon substrate was made by rubbing In–Ga eutectic in its backside (sometimes, silver epoxy was used). Cyclic voltammograms in supporting electrolyte solution (1 M KCl) were recorded at linear potential scanning at a rate of 5–100 mV s^{-1} by using a SOLARTRON 1280B electrochemical unit or a PI-50-1 potentiostat equipped with a PR-8 programming unit and a PDA x–y recorder. The potentials are given against Ag/AgCl-electrode.

Table 1 Dependence of average crystallite size, differential capacitance, and background current in 1 M KCl on the diamond film thickness

Film thickness d/μm	Average crystallite size/μm	Background current J_{BG}/μA cm^{-2}	Differential capacitance C/μF cm^{-2}
0.5	0.57 ± 0.07	10	4.94
1.4	0.75 ± 0.10	5	4.95
1.83	1.1 ± 0.03	5	3.17
2.5	–	5	3.42
3.7	–	2	3.36
4.0	2.02 ± 0.7	1	2.27

The electrochemical impedance spectra were taken over the 1–20 kHz frequency range using the SOLARTRON 1280B spectra analyzer; at higher frequencies (up to 200 kHz), by using an R-5021 ac bridge. The elements of equivalent circuit were calculated by comparing the experimentally measured impedance spectra with those calculated for the Ershler–Randles equivalent circuit comprising three elements: the diamond electrode differential capacitance C, the charge transfer resistance R_F, and the Ohmic (electrode & electrolyte) resistance. The r.m.s. error usually did not exceed 5×10^{-4} to 10^{-3}.

3 Results

In Fig. 3 we show cyclic voltammograms recorded for diamond films of different thickness, to measure the potential window width in 1 M KCl. Generally, the potential window width is typical of diamond electrodes [1], which is an evidence of rather high quality of the diamond samples. The more so, the background current is as small as a few μA cm^{-2} (Table 1), which points to the absence of pinholes even in the thinnest film ($d = 0.5$ μm). We see from Fig. 3 and Table 1 that the window width increases and the background current value gradually decreases with the increasing of the film thickness.

In Fig. 4 we give the complex-plane plots of impedance spectra (in bilogarithmic coordinates) for the 0.5–2.5 μm-thick diamond films, measured in the supporting electrolyte at the open circuit potential. Their shape and position gradually change with the increasing of film thickness. The value of differential capacitance, a few microfarads per 1 cm^2 (Table 1), is characteristic of rather heavily doped

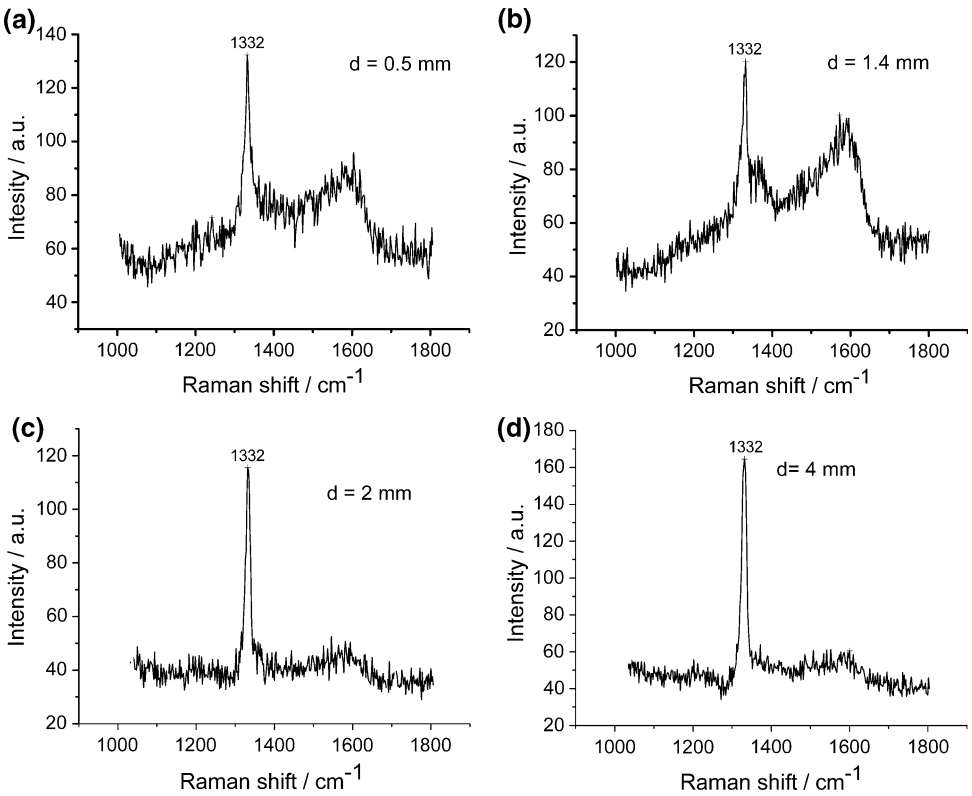

Fig. 2 Raman spectra for diamond electrodes of different thickness d (shown at the *curves*)

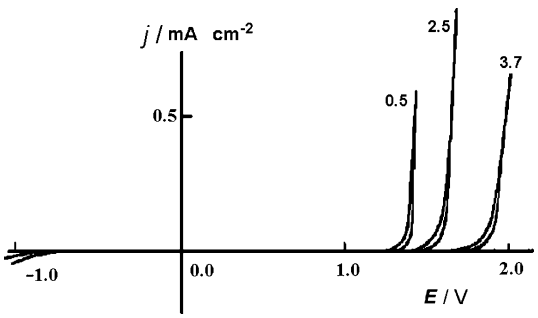

Fig. 3 Cyclic voltammograms showing the effect of film thickness on potential window width. 1 M KCl solution; potential scan rate 50 mV s^{-1}. The film thickness d (μm) is shown at the curves

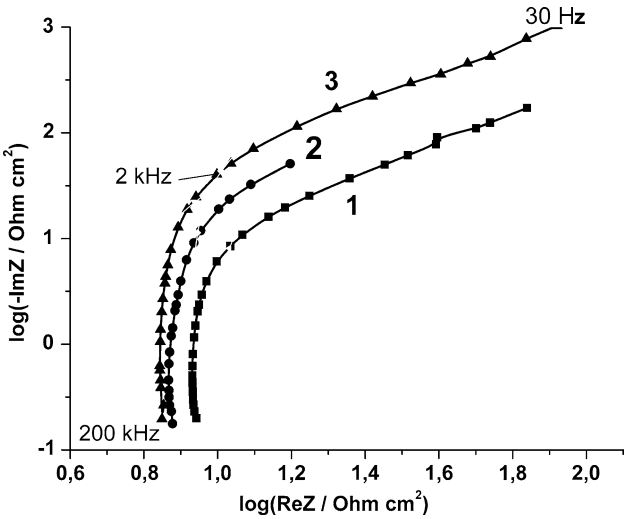

Fig. 4 Complex-plane plots of impedance spectra in 1 M KCl solution. Diamond film thickness d (μm): *1* 0.5, *2* 1.4, *3* 2.5

diamond films well suitable for using as electrodes in the electrosynthesis and electroanalysis [10, 11]. As to the effect of film thickness, we can conclude that on the whole the capacitance decreases with the increasing of the thickness d.

The effect of the diamond film thickness on the electrochemical kinetics was studied in a model redox system $[Fe(CN)_6]^{3-/4-}$ by using the electrochemical impedance spectroscopy. We determined the transfer coefficients α and β in the system, as in our earlier works [2, 3, 12], by measuring the differential capacitance in solutions containing both $K_3[Fe(CN)_6]$ and $K_4[Fe(CN)_6]$ at the equilibrium potential that sets in at the diamond electrodes. The method of the determination of α and β is based on the measuring of dependence of the exchange current j_0 in a redox solution on the concentration of one form, e.g., oxidized (c_{ox}), the other (the reduced form, c_{red}) being kept constant (or vice versa). Here we used the formula $j_0 = nFk_0\, c_{ox}^{1-\alpha}\, c_{red}^{\alpha}$ where k_0 is the reaction rate constant. The exchange current j_0 was determined from the charge transfer (Faradaic) resistance R_F measured in the redox couple solution at the equilibrium potential: $R_F = RT/(nFj_0)$. The charge transfer resistance R_F was measured as a

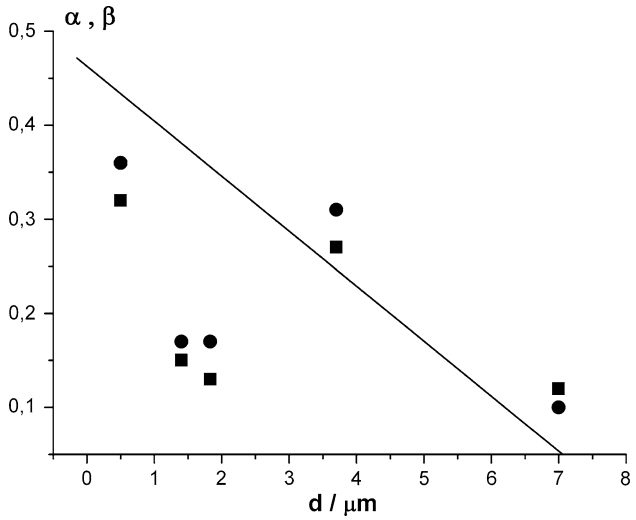

Fig. 5 Dependence of the transfer coefficients (*filled circle*) β for $[Fe(CN)_6]^{4-}$ oxidation and (*filled square*) α for $[Fe(CN)_6]^{3-}$ reduction on the film thickness

low-frequency cut-off in complex-plane plots recorded in solutions 1 M KCl + 0.1 M $K_3[Fe(CN)_6]$ + *x*M $K_4[Fe(CN)_6]$) (or 1 M KCl + 0.1 M $K_4[Fe(CN)_6]$ + *x*M $K_3[Fe(CN)_6]$).

In Fig. 5 we show the dependence of the transfer coefficients β (for $[Fe(CN)_6]^{4-}$ oxidation) and α (for $[Fe(CN)_6]^{3-}$ reduction) on the diamond film thickness *d*. Despite the scatter of points (probably caused by some second-order effect), the data reveal a well reproducible general trend: with the increasing of the film thickness *d* the transfer coefficients decrease down to $\sim$0.1, that is, the value characteristic of semiconductor electrodes and, more generally, poor conductors.

4 Discussion of results

From the above-given results we see that the thinner the diamond films, the higher is their electrochemical activity: higher are the differential capacitance and background current, the transfer coefficients in the redox-reaction approach the value characteristic of that for metal-like electrodes ($\sim$0.5).

The film-thickness dependence of the electrochemical characteristics in all probability can be explained by the contribution from nondiamond (amorphous) carbon of intercrystalline boundaries to the electrochemical properties of the polycrystalline diamond electrodes. Indeed, during diamond film growth, "strong" crystallites suppress the growing of "weak" ones. Hence, with the increasing of film thickness the number of crystallites per unit surface area decreases and the visible crystallite size at the film outer surface (the "growth" surface) increases. Correspondingly, the role of intercrystalline boundaries weakens. The intercrystalline boundaries are composed of disordered carbon that can contribute, along with the crystalline diamond, to the electrode behavior [4–6]. Another source of the nondiamond carbon is structure defects in the crystallites. Generally, the crystals become more perfect during their growth, the defect concentration decreases. On both reasons, the thicker the diamond films, the less significant is the contribution from the nondiamond carbon to the electrode behavior of the polycrystalline diamond, in particular, to the differential capacitance, transfer coefficients, and background current, which appeared very sensitive to the structure defects.

The above result agrees qualitatively with the data of Bennett et al. [13] who varied the fraction of sp^2-carbon in CVD-diamond films by changing the methane content in the feeding gas. Also, it is in accordance with the data we obtained in the studies of the two sides of a free-standing thick CVD-diamond plate [14]. Here, the growth surface of the film and the inner bulk of its adjacent well-formed diamond crystallites (sized up to 60 μm) have relatively perfect crystal structure. By contrast, at the nucleation surface and in the domain of initial growth (comprised by submicron-sized crystallites), structure defects (in particular, associated with the intercrystalline boundaries) are known to be present at a high concentration. Aiming at the elucidation of possible effect of this difference in the structural perfection on the electrochemical behavior of the diamond, we measured electrochemical parameters (in particular, differential capacitance) at the two opposite sides of the film. The obtained difference in the acceptor concentration, caused by the crystal imperfectness of the thin diamond layer formed at the initial stage of the diamond nucleation and growth, manifested itself in the different behavior of the two sides of the plate. The numerous structure defects increased the differential capacitance at the nucleation side. By contrast, at the growth side, the diamond structure is more perfect; thus, the capacitance appeared much lower.

5 Conclusions

(1) The electrochemical behavior of polycrystalline diamond films of different thickness is studied. With the increasing of the films thickness, the crystallite size increased; thus, the admixture of nondiamond (sp^2-) carbon in the intercrystalline boundaries was controlled.

(2) As the film thickness increased, both the differential capacitance and background current in the indifferent electrolyte, as well as the transfer coefficients in the $[Fe(CN)_6]^{3-/4-}$ redox system, decreased; thus, the

diamond electrodes become as if less reversible. The effect of the films' thickness is reduced to "activating" action of nondiamond (amorphous) carbon contribution from intercrystalline boundaries on the electrochemical behavior of the polycrystalline diamond electrodes.

Acknowledgment This work was supported by the Russian Foundation for Basic Research, project no. 07-03-00069.

References

1. Evstefeeva YuE, Krotova MD, Pleskov YuV, Elkin VV, Varnin VP, Teremetskaya IG (1998) Elektrokhimiya 34:1171
2. Pleskov YuV, Evstefeeva YuE, Krotova MD, Mishuk VYa, Laptev VA, Palyanov YuN, Borzdov YuM (2002) J Electrochem Soc 149:E260
3. Pleskov YuV, Evstefeeva YuE, Krotova MD, Elkin VV, Baranov AM, Dement'ev AP (1999) Diam Relat Mater 8:64
4. Duo I, Fujishima A, Comninellis Ch (2003) Electrochem Commun 5:695
5. Mahé E, Devilliers D, Comninellis Ch (2005) Electrochim Acta 50:2263
6. Martin HB, Argoitia A, Landau U, Anderson AB, Angus JC (1996) J Electrochem Soc 143:L133
7. Ohnishi K, Einaga Y, Fujishima A (2000) In: Abstracts, 4th Int Mini-Symp on Diamond Electrochemistry and Related Topics, Tokyo, p 43
8. Chen Q, Gruen DM, Krauss AR, Corrigan TD, Witek M, Swain GM (2001) J Electrochem Soc 148:E44
9. Pleskov YuV, Krotova MD, Elkin VV, Ralchenko VG, Saveliev AV, Pimenov SM, Lim P-Y (2007) Electrochim Acta 52:5470
10. Pleskov YuV (2003) Electrochemistry of diamond (in Russian). Editorial URSS, Moscow
11. Fujishima A, Einaga Y, Rao TN, Tryk DA (eds) (2005) Electrochemistry of diamond. BKC, Elsevier, Tokyo, Amsterdam
12. Modestov AD, Pleskov YuV, Varnin VP, Teremetskaya IG (1997) Elektrokhimiya 33:60
13. Bennett JA, Wang J, Show Y, Swain GM (2004) J Electrochem Soc 151:E306
14. Pleskov YuV, Evstefeeva YuE, Krotova MD, Ralchenko VG, Vlasov II, Loubnin EN, Khomich AV (2003) J Appl Electrochem 33:909